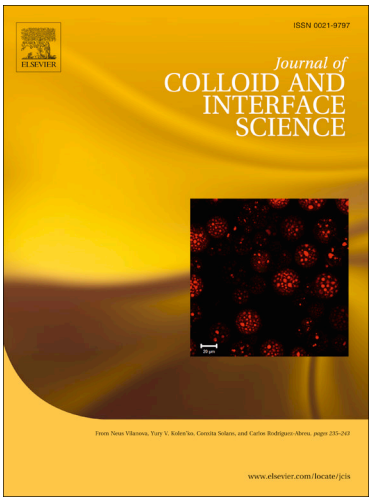

Nonlinear Electrokinetic Motion of Electrically Induced Janus Droplets in Microchannels

Mengqi Li, Dongqing Li

PII: S0021-9797(18)31424-3
DOI: https://doi.org/10.1016/j.jcis.2018.11.102
Reference: YJCIS 24367

To appear in: *Journal of Colloid and Interface Science*

Received Date: 18 September 2018
Accepted Date: 26 November 2018

Please cite this article as: M. Li, D. Li, Nonlinear Electrokinetic Motion of Electrically Induced Janus Droplets in Microchannels, *Journal of Colloid and Interface Science* (2018), doi: https://doi.org/10.1016/j.jcis.2018.11.102

Nonlinear Electrokinetic Motion of Electrically Induced Janus Droplets in Microchannels

Mengqi Li and Dongqing Li*

Department of Mechanical and Mechatronics Engineering, University of Waterloo, Waterloo, Ontario, Canada N2L 3G1

*Corresponding author, Address: 200 University Ave. West, Waterloo, Ontario, N2L 3G1
Email: dongqing@uwaterloo.ca (D. Li)

Electronic supplementary information (ESI) is available.

Abstract

The nonlinear electrokinetic motion of electrically induced Janus droplets (EIJDs) in a microchannel is studied in this paper. The EIJDs were fabricated by operating the positively charged aluminum oxide nanoparticles to partially cover the oil droplets with electric field. The nanoparticle coverage of the EIJDs changes with the electric field strength, which leads to the variation of the electrophoretic mobility of the EIJDs. Therefore, the electrokinetic velocity of the EIJDs in a microchannel changes nonlinearly with the electric field strength. In this research, the variations of the nanoparticle coverage under both constant and time-varying electric fields were studied. The results indicate that the nanoparticle coverage of the EIJDs decreases with the increase of the electric field strength. Based on the experimental results, an empirical equation for calculating nanoparticle coverage as a function of the electric field was derived. Under time-varying electric field, the variation of nanoparticle coverage lags behind the change of electric field, and the nanoparticle coverage changes differently under different time-varying electric fields. The experimental results of the electrokinetic motion of the EIJDs in a microchannel confirm that the electrokinetic velocity increases nonlinearly with the electric field. Due to the lag of the nanoparticle coverage, the variation of the electrokinetic velocity in a microchannel is different between the increasing and decreasing periods of the electric field.

Keywords: Electrokinetic motion; electrically induced Janus droplet; aluminum nanoparticle; microchannel; electric field.

1. Introduction

As one of the electrokinetic phenomena, electrophoresis has been used as an efficient analytical technique in many fields, such as biomedical science[1,2], biochemistry[3–5] and colloidal science[6,7]. For example, Huang et al. [4] separated different size DNA molecules successfully in a micro-post array based on the electrophoresis of the DNA molecules. By applying asymmetric pulsed electric fields, the DNA molecules with different sizes undergo different electrophoretic velocities in the array and are sorted in different directions. Generally, for a uniformly charged particle with a thin electric double layer (EDL), the electrophoretic velocity of the particle in a bulk stationary liquid (v_{ep}) is proportional to the strength of the externally applied electric field (E), which is given by the well-known Helmholtz-Smoluchowski equation[8]:

$$v_{ep} = -\frac{\varepsilon_0 \varepsilon_m}{\mu} \zeta_p E = -\mu_{eph} E \tag{1}$$

where ε_0 and ε_m are the permittivity of vacuum and the bulk liquid, respectively. μ is the viscosity of the liquid, ζ_p is the zeta potential of the particle, and μ_{eph} is called the electrophoretic mobility. When the particle is injected into a microchannel, the motion of the particle results from both the electrophoresis of the particle and the electroosmotic flow (EOF) of the bulk liquid in the microchannel. The velocity of the electrokinetic motion, v_{ek}, is characterized by[9]:

$$v_{ek} = -\frac{\varepsilon_0 \varepsilon_m}{\mu} (\zeta_w - \zeta_p) E \tag{2}$$

where ζ_w is the zeta potential of the microchannel wall. According to Eq. (2), the electrokinetic velocity of the charged particle also has linear relationship with the electric field.

For the electrophoresis of droplets with uniformly surface charges, both experimentally and theoretically studies have been reported extensively. Theoretically, Booth [10] first derived a formula for the electrophoretic velocity of charged droplets in terms of the applied electric field by retaining spherical shape of the droplets and neglecting the retardation effect. However, the formula disagrees with the experimental findings[11]. Later, Baygents and Saville [12] studied the electrophoresis of non-conducting droplets. They found that the liquid droplet performs as solid particle with the adsorption of ionic solutes and polarization. The expression of the

electrophoretic mobility of a droplet in a salt-free medium was derived by Ohshima [13], which is a function of the size, viscosity and zeta potential of the liquid droplet. Experimentally, the effects of the concentration of surfactant, pH value and ion strength on the electrophoresis of charged oil droplets were studied in some published papers, respectively [14–17]. Overall, the concentration of surfactant, pH value and ion strength affect the electrophoretic motion by changing the zeta potential of the oil droplets. While keeping the above-mentioned parameters fixed, the electrophoretic mobility remains a constant value regardless of the electric field strengths; therefore, the electrophoretic velocity increases proportionally with the electric field strength.

In the last decade, with the development of microfabrication technologies, the Janus particle/droplet with two segments carrying different properties has been made. Some studies have emerged to test the electrophoresis of the anisotropic particle/droplet. For non-conducting solid Janus particles, Anderson [18] theoretically studied the electrophoresis with the assumption of thin EDL. By considering the force and torque balance, the analytical expressions of the translational and rotational velocities of the Janus particle was derived. Based on Anderson's theory, the electrophoretic mobility is determined by the particle's area-average zeta potential. Later, with the same assumption, the analysis of non-spherical ellipsoidal Janus particles was carried out by Fair and Anderson [19]. The electrophoretic motions of spherical and cylindrical Janus particles in confined regions, such as a spherical cavity, were studied by Hsieh and Keh [20,21]. It was found that with the presence of the confining wall, the viscous retardation effect of the moving particles increases; hence, the electrophoretic motion of the Janus particles was affected. With numerical method, Hsu et al. [22] studied the electrophoresis of Janus particles with arbitrary double layer thickness. For Janus particles with thick EDL, the double-layer polarization (DLP) effect becomes significant, which leads to the reduction of electrophoresis. Qian et al. [23] studied the electrokinetic motion of a Janus nanoparticle in a nanotube by building up a multi-physics model. The results indicated that the electrophoretic motion of the Janus nanoparticle is dependent on the surface charge distribution of the nanoparticle. In addition to non-conducting solid Janus particles, the electrophoresis of metal-dielectric Janus particles were also analyzed [24–31]. Under electric field, induced-charge electroosmosis (ICEO) can be generated on the metallic side and vortices show up around the Janus particle. As a result, the electrophoretic motion direction of the Janus particle in a free (infinitely large) solution is always

toward the dielectric side [27,28]. In a microchannel, the induced vortices around the Janus particle perform as "engines"; therefore, the electrophoretic velocity of Janus particle is larger than the other homogeneous particles[29–31]. Daghighi et al. [31] measured the electrokinetic velocity of nickel-polystyrene Janus particles under different electric field strengths in a microchannel. Due to the polarization limit of the conducting hemisphere of the Janus particle, the measured electrophoretic velocity of the particle changes nonlinearly with the electric field.

The studies on the electrophoresis of Janus droplets were limited. In our previous studies, a novel method was developed to generate electrically induced Janus droplets (EIJDs) with positively charged alumina (Al_2O_3) nanoparticles under electric field [32,33]. The Janus droplets fabricated with this method are partially covered with Al_2O_3 nanoparticle films. In deionized water, the nanoparticle film and the oil-water interface carrying surface charges of the opposite signs. The electrokinetic motion of the EIJDs in a microchannel was studied both theoretically and experimentally[34,35]. In these studies, the effects of droplet size, nanoparticle coverage and strength of electric field were studied, respectively. As all of the analyses were conducted under relatively high electric field (larger than 50 V/cm), the nanoparticles adhering on the droplets are compacted and the nanoparticle coverage of the Janus droplets remains constant, regardless of the different electric field strengths. Hence, the electrophoretic mobility of the EIJDs is fixed that the electrokinetic velocity of the EIJDs increases proportionally with the electric field. However, this condition, fixed nanoparticle coverage, is inapplicable under relatively weak electric field. The nanoparticle coverage of the Janus droplets changes significantly with the strength of the electric field under weak electric field. Therefore, the electrophoretic mobility of the Janus droplet varies with electric field, which leads to nonlinear relationship between the electric field and the electrokinetic velocity.

In this paper, nonlinear electrokinetic motion of the EIJDs in a microchannel was studied under both constant and time-varying electric fields. The variation of nanoparticle coverage of EIJDs with electric field strengths was investigated first, and an empirical equation was obtained from the experimental results. Then, the lag of the variation of nanoparticle coverage of the EIJDs behind the change of electric field was characterized by measuring the evolution time of the nanoparticle film under different electric field strengths and by comparing the variations of nanoparticle coverage under different time-varying electric fields. In the study of the

electrokinetic motion of the EIJDs in a microchannel, the electrokinetic velocities of the EIJDs under different electric field strengths and different time-varying electric fields were measured, respectively.

2. Experimental section

2.1 Preparation of Al_2O_3 nanoparticle suspensions

The aluminum oxide nanoparticle suspension was obtained by dispersing the Al_2O_3 nanoparticles into water with ultrasonic treatment. The following procedure was used: a) place a certain amount of Al_2O_3 nanoparticles (US Research Nanomaterials Inc., 18 nm in average diameter), into a glass vial; b) drop deionized water of 5 mL (18 MΩ·cm, Milli-Q, Japan Millipore, Japan) into the vial; c) add 100 μL Tween 20 (Sigma-Aldrich) into the mixture. Tween 20 is nonionic surfactant, which serves as dispersant to enhance the dispersion stability of nanoparticles; d) put the glass vial in an ultrasonic clearer (Cody Technology Limited Co.). After the ultrasonic treatment of 8 min, the nanoparticles were dispersed into the water phase and nanoparticle suspension was generated, as shown in **Figure 1(a)**.

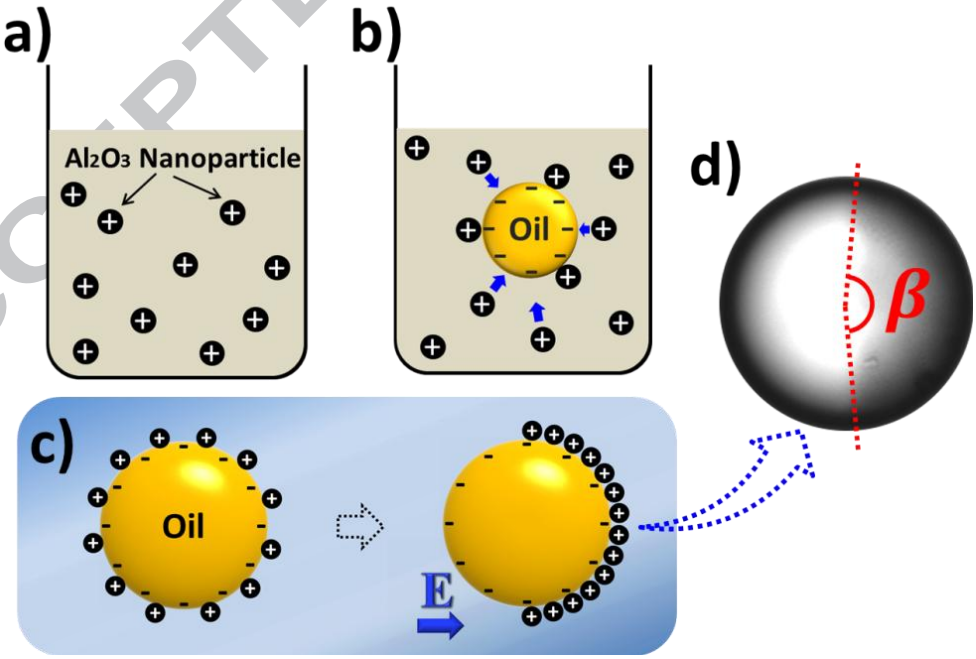

Figure 1. (a) Schematic diagram of the Al_2O_3 nanoparticle suspension; **(b)** the fabrication process of Al_2O_3 nanoparticle-stabilized Pickering emulsion droplet; **(c)** the generation of EIJD from Pickering emulsion droplet under electric field; **(d)** the microscope image of EIJD.

2.2 Preparation of suspended oil droplets

The suspended oil droplets were prepared by emulsifying oil (canola oil, 100% pure, Mazola Corporation) into continuous water phase, which includes the following steps: a) adding 1 mL of canola oil, 5 mL deionized water, 100 µL Tween 20 into a glass vial; b) vibrating the sample with a lab dancer (VWR International) for 2 min at the speed of 3200 rpm. After the emulsification process, let the emulsification stand for 24 h, and the oil droplets floated to the top layer by buoyancy.

2.3 Preparation of Al_2O_3 nanoparticle-stabilized Pickering emulsion

The Al_2O_3 nanoparticle-stabilized Pickering emulsion was prepared by immersing oil droplets into the Al_2O_3 nanoparticle suspension. 500 µL emulsion droplets were sucked from the top layer of the oil-water emulsion carefully with a digital pipette, and added into the nanoparticle suspension. Then, the mixture was vibrated with the lab dancer for 2 min at medium speed (approximately 1600 rpm). In deionized water, the surface of the oil droplets are negatively charged, while the Al_2O_3 nanoparticles carry positive charges; therefore, after adding oil droplets into the suspension, nanoparticles attach on the oil droplets to form Pickering emulsion droplets, as shown in **Figure 1(b)**. The vibration process is essential for making the oil droplets uniformly coated with nanoparticles. After this, leave the emulsion standing for one day to separate the Pickering emulsion droplets and extra nanoparticles in water through gravity. The droplets floated to the top to form a black layer while the nanoparticles sank to the bottom.

2.4 Preparation of EIJDs

The EIJDs can be formed easily by applying direct current electric field to the Al_2O_3 nanoparticle-stabilized Pickering emulsion droplets. As shown in **Figure 1(c)**, after applying an electric field, the nanoparticles attaching on the droplet surface move and accumulate to one side of the droplet. Because of the accumulation of the nanoparticles, the nanoparticle film forms on the oil droplet while leaving the other side without the presence of nanoparticle. In this study, as

the positively charged alumina nanoparticles were employed, the EIJD therefore has one side with a positively charged nanoparticle film and another side with a negatively charged oil-water interface in deionized water. The microscopic image of an EIJD is shown in **Figure 1(d)**. The dark region is coated with the nanoparticle film.

To study the variation of nanoparticle coverage of the EIJDs with the strength of electric field, nanoparticle suspensions with different concentrations of nanoparticle, 0.5 mg/mL, 1 mg/mL and 1.5 mg/mL, were formed for generating Pickering emulsion droplets and then fabricating EIJDs, respectively. Generally, as the concentration of the nanoparticle suspension increases, more nanoparticles will adhere on the droplet; therefore, the nanoparticle coverage of the EIJDs becomes larger under the same electric field.

2.5 Fabrication of microfluidic chip

The microfluidic chip was prepared with soft lithography method. In brief, a master with the designed patterns was structured first by following the processes of spin-coating, baking, exposuring and developing. After the master was fabricated, the pattern was duplicated by pouring PDMS-curing agent mixture (10:1, w/w, Sylgard 184, Dow Corning) onto it and heating at 80 ℃ for 1 h. After peeling off the cured PDMS layer from the master, and the microfluidic chip was formed by bonding the PDMS layer onto a glass substrate (VWR, VWR International) following plasma treatment (Harrick Plasma).

In the study of the effect of the electric field strength on the nanoparticle coverage of EIJDs and the electrokinetic velocity of EIJDs, a straight microchannel was designed and fabricated. The schematic diagram of the microchannel is shown in **Figure 2(a)**. The size of the channel is 1 cm × 500 μm (length × width) with its two ends connecting to the confinement chamber and the outlet, respectively. The confinement chamber is circular with the diameter of 8 mm for holding the emulsion droplets. An inlet well is punched on the confinement chamber. While studying the nanoparticle coverage, the target EIJD should remain stationary for measurement. Therefore, to block the movement of EIJD under electric field, a pair of circular pillars (25 μm in diameter) is set in the downstream of the channel, as labelled in **Figure 2(a)**. The center-to-center distance between the two pillars is 60 μm. The height of the microchannel is 80 μm.

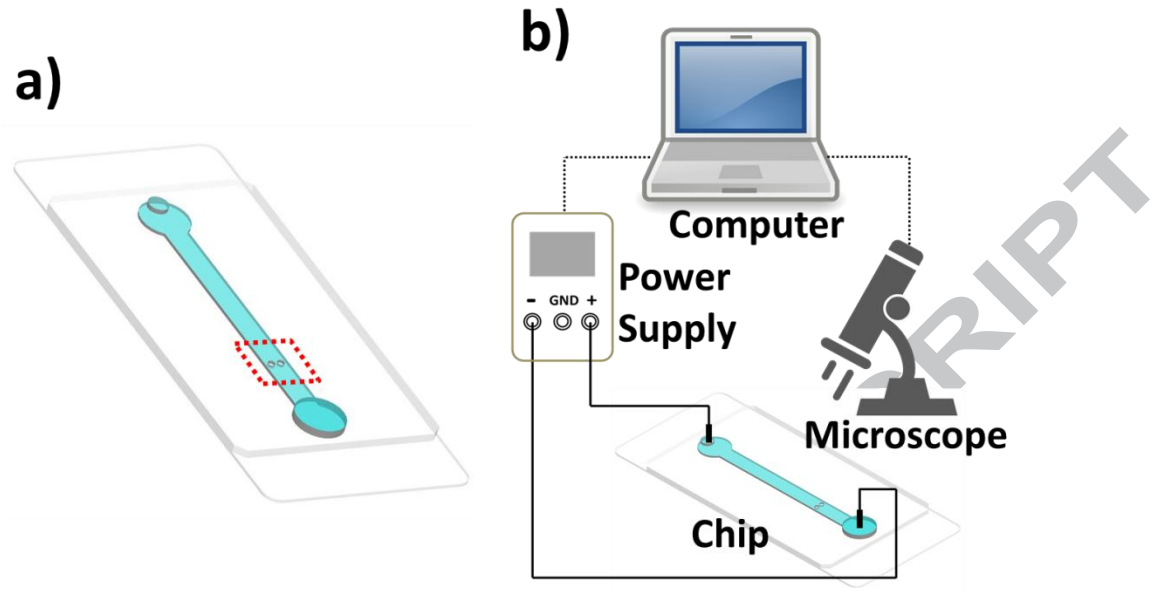

Figure 2. (a) Schematic diagram of the structure of the microfluidic chip; **(b)** schematic diagram of the experimental setup.

2.6 Analysis of nanoparticle coverage evolution with electric fields

For detecting the change of the nanoparticle coverage of the EIJDs with electric field, a simple experimental setup was used, as shown in **Figure 2(b)**. The experimental setup consists of a microfluidic chip, a direct-current (DC) power supply, a bright-field microscope (Nikon Ti-E) and a computer. The electric field was provided by the DC power supply through two platinum electrodes, the strength of which is adjustable by changing the output voltages of the power supply. The nanoparticle coverage variation of EIJDs was monitored by the microscope, and the images were recorded and sent to the compute by a charge-coupled device (CCD) camera. Under a bright-field microscope, the nanoparticle coated side of the EIJDs is black, while the other side without the presence of nanoparticle indicates as white. The two segments of EIJDs can be distinguished easily from the recorded images. As shown in **Figure 1(d)**, by using imaging analysis software, the angle between two edge lines of the nanoparticle film (β) can be measured; hence, the nanoparticle coverage of EIJDs (θ) can be calculated with following equation:

$$\theta = \frac{1-cos\beta}{2} \quad (3)$$

In the experiments, the microchannel was wetted first by adding deionized water of 10 μL into the outlet. Then, 5 μL Al_2O_3 nanoparticle-stabilized emulsion droplets were added through the confinement chamber. Following this, deionized water of 50 μL was added into the inlet well. Due to the liquid level difference between the inlet well and the outlet well, the droplets was driven to move into the main channel, and one of the droplets can be trapped by the pillars in the downstream of the channel. Afterwards, the liquid level of the wells was balanced carefully by dropping deionized water into the outlet well gradually. The electric field was applied by a power supply through the electrodes inserted in the wells. In the studies of the effect of the electric field strength on the nanoparticle coverage at steady state and the evolution time of the nanoparticle film under different electric field strengths, four serially connected DC power supplies (CSI12001X, Circuit Specialist Inc.) were employed to provide the voltage. In the study of the variation of nanoparticle coverage under time-varying electric fields, the pulsed electric fields were generated with a programmable power supply (BK Precision 1698, Yorba Linda, USA). In the experiments, the images of EIJDs were taken continuously by the microscope for later measurement and calculation.

2.7 Measurement of electrokinetic velocity

The electrokinetic velocities of EIJDs under different electric fields in a microchannel were determined by measuring the moving distance of EIJDs within a certain time interval. Briefly, the electric field, directed from inlet well to outlet well, was applied to the trapped droplet to fabricate EIJD. After this, the direction of the electric field was switched, directed from outlet well to inlet well, to drive the EIJD moving away from the pillars. As the EIJD is electrically anisotropic, with the switching of the electric field, the EIJD rotates to make its nanoparticle coated side backward the electric field constantly. Following this, the electrokinetic motions of the EIJD in the upstream of the microchannel under different electric fields were recorded at a rate of 25 frames/s. By analyzing the recordings, the electrokinetic velocities of the EIJDs were obtained finally. The electrokinetic velocities of EIJDs in both directions (towards both inlet well and outlet well) were measured, respectively, to eliminate the hydrostatic pressure effect. In the studies of the electrokinetic motion of EIJDs under different electric field strengths, four serially connected DC power supplies were employed to provide the voltage. While in the study of the

electrokinetic motion of EIJDs under time-varying electric fields, the programmable power supply was used to generate time-varying electric fields. To indicate the effect of time-varying electric field on the electrokinetic motion, pulse electric fields with different variation speed were applied to the microchannel.

3. Results and discussion

3.1 Variation of nanoparticle coverage of EIJDs with electric field

The electric field affects the nanoparticle coverage of EIJDs by changing the distances between nanoparticles attached on the droplet surface. The separation distance between two spherical nanoparticles can be predicted with the well-known DLVO (Derjaguin-Landau-Verwey-Overbeek) theory [36–41]. Based on the DLVO theory, without the presence of externally applied electric field, the interaction between two nanoparticles is composed of the Van der Waals (vdW) interaction and the electric double layer (EDL) interaction, as shown in **Figure 3(a)**. The Van der Waals force (F_{vdW}) is attractive force which trends to drag the nanoparticles together, while the EDL interaction force (F_{EDL}) is repulsive force towards the opposite direction. The variations of F_{vdW}, F_{EDL} and the total force (F_{total}, $F_{total} = F_{vdW} + F_{EDL}$) with the distance between two nanoparticles are shown in **Figure 3(c)**. As shown in this figure, the steady state is reached at point A, where the total force is equal to zero. After applying electric field from left to right, the electrostatic force, F_e, exerts on the positively charged nanoparticles, which is toward the cathode of the electric field. As shown in **Figure 3(b)**, the direction of F_e is identical to that of the attractive Van der Waals force. With the presence of F_e, the balance between the F_{vdW} and F_{EDL} is broken, the two nanoparticles move closer to each other until a new force balance is reached. The final distance between the two nanoparticles is determined by the strength of the externally applied electric field. Generally, as the strength of the electric field increases, the distance decreases to generate equivalent repulsive F_{total} to balance the electric force, as shown in **Figure 3(c)**. However, as F_{total} decreases sharply with the distance, the further increase of electric force only leads to limited decrease of the separation distance.

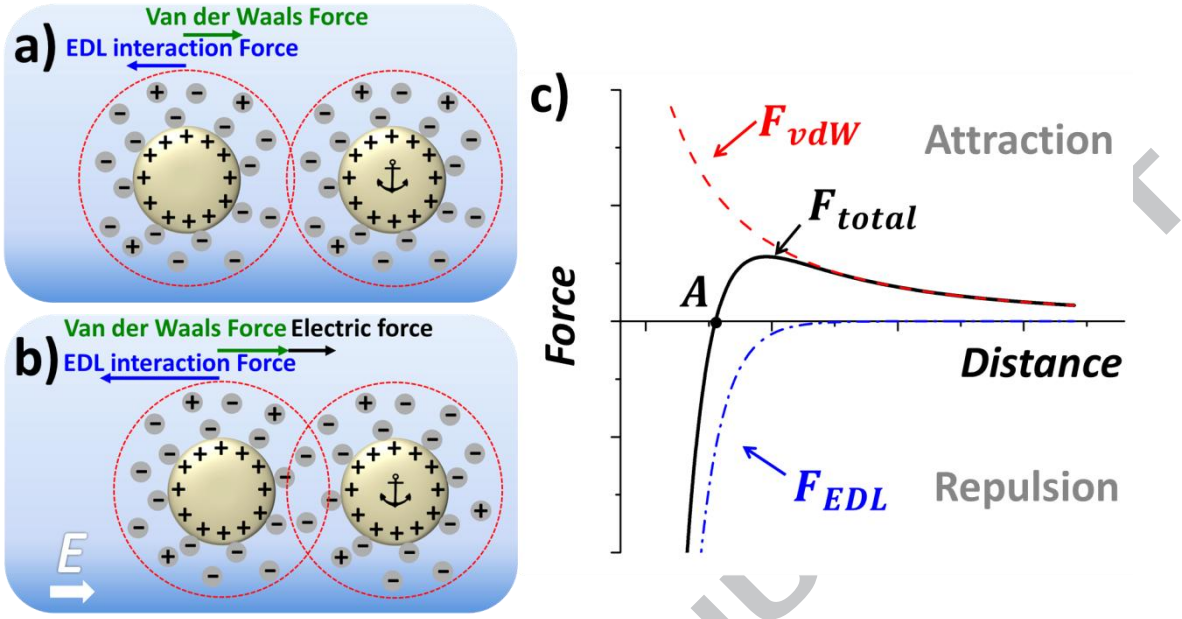

Figure 3. (a)-(b) Schematic diagrams of the forces acting on the left nanoparticle with **(b)** and without **(a)** the presence of electric field. The right nanoparticle gets anchored, while the left one is free to move. **(c)** Schematic diagram of the variation of Van der Waals Force, EDL interaction force and total force with the distance between two nanoparticles.

The variation the nanoparticle coverage of the EIJDs with the electric field strength is shown in **Figure 4**. As an example, the microscope images of the EIJD formed from 1 mg/mL nanoparticle suspension under different electric fields are presented in **Figure 4(a)**. As indicated in the serial images, with the increase of the electric field strength, the area of the nanoparticle film decreases. The variation of the nanoparticle coverage is significant under relative weak electric field, ranging from 10 V/cm to 50 V/cm. Once the electric field becomes larger than 50 V/cm, further increasing of the electric field only leads to very limited area reduction of the nanoparticle film. The video showing the variation of the area of nanoparticle film of EIJD is available in the ESI (Supplementary Movie 1). To characterize the relationship between electric field strength and the nanoparticle coverage of EIJDs quantitatively, the nanoparticle coverages of EIJDs fabricated from different concentrated nanoparticle suspensions were measured under different electric fields. Three typical examples of the variation of nanoparticle coverage of

EIJDs (θ) in terms of of the strength of electric field (E) are plotted in **Figure 4(b)**. It is clearly shown in this figure that for all of the three EIJDs carrying different amount of nanoparticles, both θ and the variation rate of θ decreases as E increases. Under the electric field of 10 V/cm, the nanoparticle coverage of the EIJD generated from 1 mg/mL (indicated by red rectangular points in **Figure 4(b)**) is around 50 %. When E increases to 50 V/cm, θ reduces to 38 %. However, with the further increase of the electric field from 50 V/cm, θ almost remains constant which only decreases from 38 % to 35 %. This phenomenon can be understood based on the DLVO theory shown above. Under an externally applied electric field, the extra electrostatic force applies to the nanoparticles and the nanoparticles get redistributed by moving closer to each other; therefore, the nanoparticle coverage of the EIJDs decreases. However, as the repulsion force increases sharply with the smaller separation distance between nanoparticles, the reduction of the separation distance between nanoparticles decreases under high electric field; hence, the variation rate of the nanoparticle coverage decreases with the further increase of the electric field.

In describing the relationship between nanoparticle coverage and electric field quantitatively, two normalized parameters, relative coverage (θ_r) and relative electric field (E_r), were introduced:

$$\theta_r = \frac{\theta}{\theta_{@10\ V/cm}} \tag{4}$$

$$E_r = \frac{E}{10\ V/cm} \tag{5}$$

where $\theta_{@10\ V/cm}$ is the nanoparticle coverage of the EIJDs under electric field of 10 V/cm. Based on Eq. (4) and (5), both the nanoparticle coverage and the electric field are normalized. The variation of θ_r as a function of E_r was plotted in **Figure 4(c)**, and an empirical equation was derived to give the relationship between nanoparticle coverage and electric field strength:

$$\theta_r = 0.66 + 0.41 \times 0.84^{E_r} \tag{6}$$

The adjusted coefficient of determination between the experimental results and the empirical equation is 0.998, which allows for accurate and precise prediction of θ_r with the empirical equation. As shown in **Figure 4(c)**, based on the reduction rate of θ_r, the variation of θ_r can be

divided into two stages: a sharp descent stage (Ⅰ) and a gentle descent stage (Ⅱ). In the first stage, E_r ranges from 0 to 5, and the decline of θ_r is significant with the increase of E_r. For E_r larger than 5, the second stage is reached. In this stage, the variation of θ_r is limited and θ_r approaches a constant with the increase of E_r. The EIJDs with the diameter ranging from 50 μm to 75 μm were chosen.

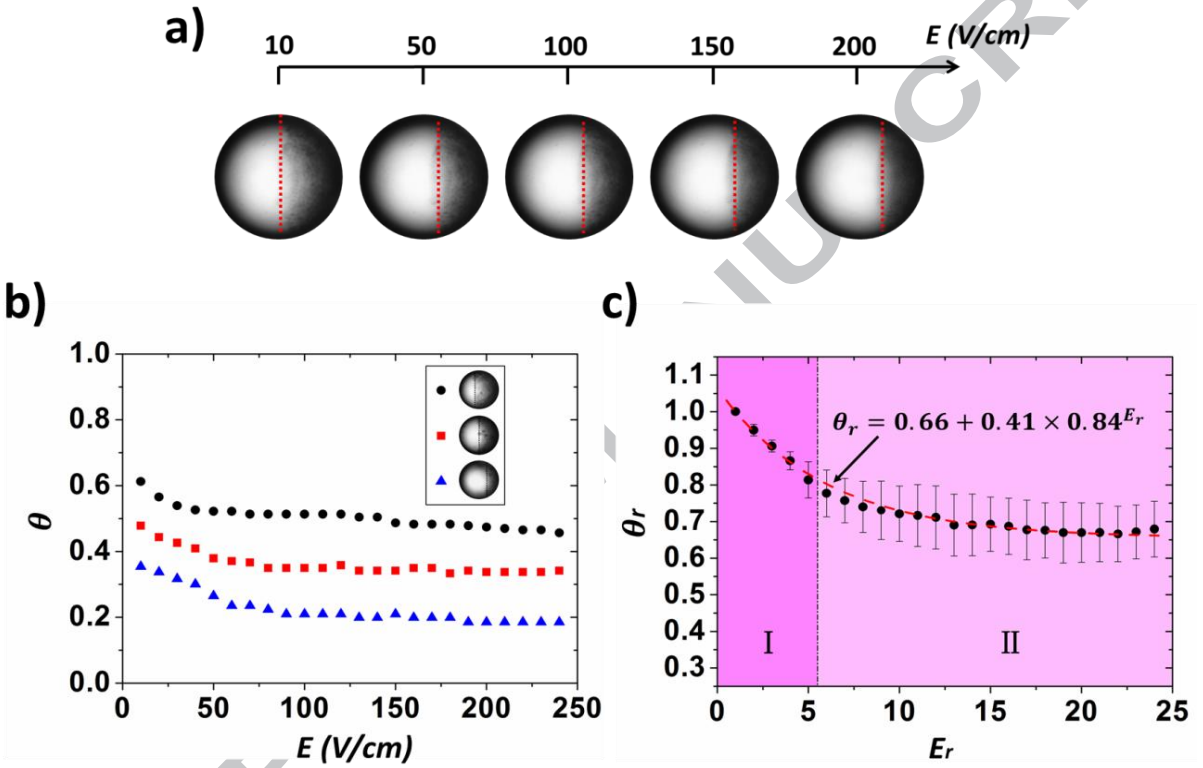

Figure 4. (a) Microscope images of the EIJD fabricated from 1 mg/mL nanoparticle suspension under different electric field strengths; **(b)** three typical examples of the variations of nanoparticle coverage as a function of the electric field strength for the EIJDs carrying different amount of nanoparticles. The circular point, rectangular point and triangular point refer to the EIJDs generated from 1.5 mg/mL, 1 mg/mL and 0.5 mg/mL nanoparticle suspensions, respectively; **(c)** the variation of relative coverage, θ_r, with the relative electric field, E_r. The diameters of the EIJDs range from 50 μm to 75 μm.

3.2 Evolution time of the nanoparticle film

After applying electric field to the Al_2O_3 nanoparticle-stabilized Pickering emulsion, electrostatic forces are exerted on the nanoparticles, and the nanoparticles undergo electrokinetic motion on the oil droplets. The moving direction of the nanoparticles is identical to that of the electric field. The moving velocity of the nanoparticles depends on the electric field [42]. Generally, as the electric field strength increases, the velocity of the nanoparticles increases. Furthermore, as shown above, the variation rate of the nanoparticle coverage and hence the moving distance of the nanoparticles decrease with the further increase of the electric field when the applied electric field becomes relatively higher. Due to the combined effects of the increased velocity and the decreased moving distance, the evolution time of the nanoparticle film decreases with the increase of the electric field.

To study the effect of the electric field on the evolution time of the nanoparticle film of the EIJDs, the electric field applying to the EIJDs was increased gradually from 10 V/cm to 50 V/cm with the interval of 10 V/cm. Under a given electric field strength, the variation of the nanoparticle film was recorded, and the evolution time was measured with the recorded videos. The variation of the evolution time with the electric field is plotted in **Figure 5**. As shown in this figure, the time decreases significantly with the increase of the strength of the electric field. Initially, with E = 10 V/cm, it takes approximately 35 s for the nanoparticles to accumulate to the steady state. However, when E increases to 50 V/cm, only 5 s is needed for the EIJDs to reach the steady state. The video showing the evolution of the nanoparticle film of an EIJD with the electric field is available in the ESI (see Supplementary Movie 2). It should be noted that, the evolution time of nanoparticle film of the EIJDs were measured and analyzed only in the electric field increasing period. As shown in Supplementary Movie 2, when the electric field starts to decrease gradually from 50 V/cm, the nanoparticle coverage changes very slowly, and the nanoparticles get dispersed quickly only under weak electric field (smaller than 10 V/cm). Therefore, it's hard to measure the evolution time of the nanoparticle film in the decreasing period of the electric field.

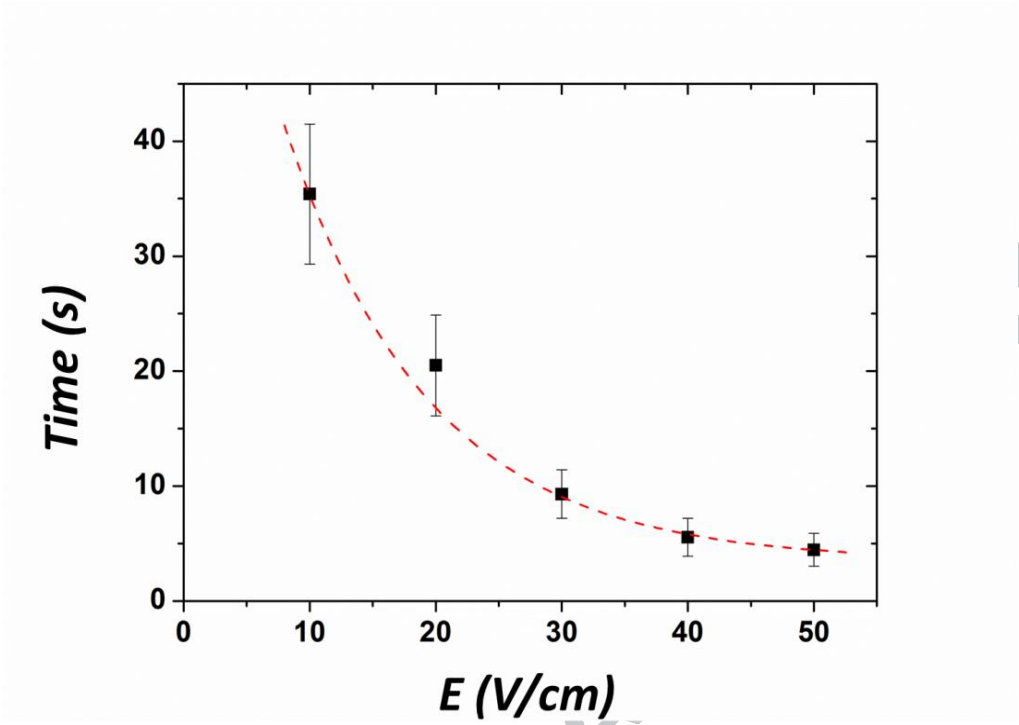

Figure 5. Effect of the strength of the electric field on the evolution time of the nanoparticle film of the EIJDs. The diameters of the EIJDs range from 50 μm to 75 μm. The EIJDs are formed from 1 mg/mL nanoparticle suspension.

3.3 Variation of nanoparticle coverage of EIJDs under time-varying electric field

The variation of nanoparticle coverage of the EIJDs is different under different time-varying electric fields. As the evolution of the nanoparticle film of the EIJDs takes time, the variation of nanoparticle coverage lags behind the variation of the electric field. The lag of the variation of nanoparticle coverage is dependent on the speed of the electric field. Generally, the faster the variation speed of the electric field, the more significant the lag of the nanoparticle coverage variation. The variations of the nanoparticle coverage of an EIJD under different time-varying electric fields are shown in **Figure 6(a)**, **(b)** and **(c)**, respectively. The electric fields are pulsed, which increase from 0 to 50 V/cm then decrease to 0 within a time period t. As shown in these figures, the variation of θ (nanoparticle coverage) is different between the increasing and the decreasing periods of the electric field. Under the same strength of electric field, θ in the

increasing period is larger than that in the decreasing period. This is because that, in comparison to the accumulation of the nanoparticles in the electric field increasing period, the dispersion of the nanoparticles with the decrease of the electric field is very slow. Hence, the lag of the variation of θ is more significant in the decreasing process. To make convenient comparison, the fitting curves of θ under the time-varying electric fields with t = 20 s, 40 s and 60 s are plotted in the same figure (**Figure 6(d)**). As shown in this figure, with the decrease of t, the lag of θ becomes more significant. As a result, in the increasing process (the upper side of each curve), θ increases with the decrease of t under the same electric field strength. For the decreasing process, the variation trend is adverse that θ decreases with t. It should be noted that, to make accurate comparison, the same EIJD was employed and analyzed under the three different electric fields. 5 measures were conducted at each point to get the average nanoparticle coverage and the standard deviation.

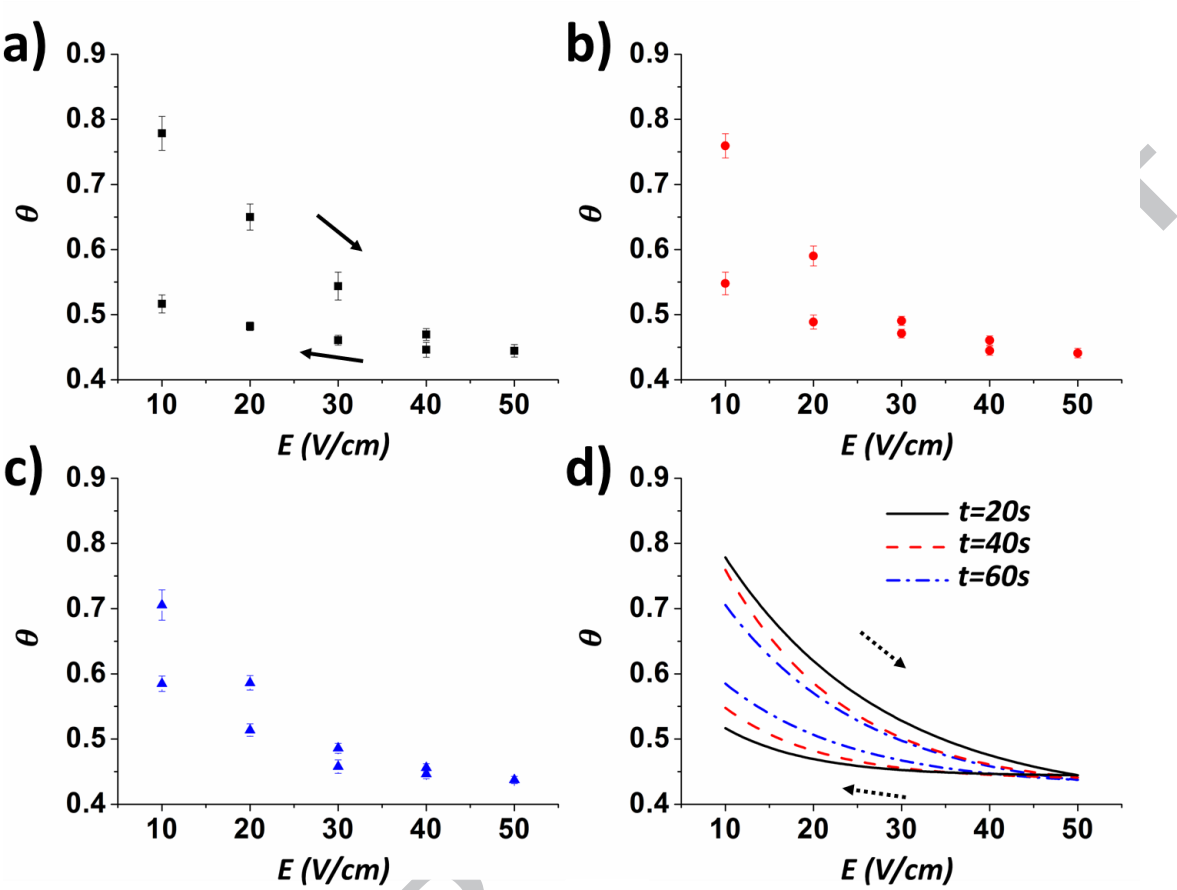

Figure 6. (a)-(c) The variation of nanoparticle coverage under different time-varying electric fields with t = 20 s **(a)**, t = 40 s **(b)** and t = 60 s **(c)**. **(d)** The fitting curves of θ under different time-varying electric fields. The EIJD is developed from 1 mg/mL nanoparticle suspension with the diameter of approximately 70 μm.

3.4 Electrokinetic motion of EIJDs in a microchannel

The electrokinetic motion of EIJDs in a microchannel is determined by the effects of the electrophoresis (EP) of the EIJDs and the electroosmotic flow (EOF) in the microchannel. Generally, for the droplets with fixed topology, both the EOF and EP have linear relationship with the electric field strength; therefore, the combined electrokinetic velocity increases proportionally with the electric field. However, for the EIJDs, the nanoparticle coverage changes with the electric field. This leads to nonlinear variation of the electrokinetic velocity of the EIJDs

with the electric field. The experimentally measured electrokinetic velocities of EIJDs generated by using 1 mg/mL nanoparticle suspension under different electric fields are shown in **Figure 7**. As shown in this figure, the measured electrokinetic velocity increases with the electric field strength. When the electric field increases from 30 V/cm to 50 V/cm, the EOF in the microchannel increases with the electric field while the nanoparticle coverage of the EIJDs decreases significantly. When the electrophoresis of the EIJD is weaker than the EOF in the microchannel, the EIJD will carried by the EOF to move with the surrounding liquid. The increasing EOF leads to the increases of the electrokinetic velocity of EIJDs. The electrophoretic mobility is the ratio between the electrophoretic velocity and the electric field strength, as indicated in Eq. (1). For an EIJD with surface area S and nanoparticle coverage of θ, the electrophoretic mobility of the EIJD is related to its average zeta potential ($\bar{\zeta}$). The average zeta potential of the EIJD is obtained by [18]:

$$\bar{\zeta} = \frac{1}{S}\int \zeta_0 dS = \zeta_{ow} \cdot (1-\theta) + \zeta_{nano} \cdot \theta \qquad (7)$$

where, ζ_0 is the local zeta potential, ζ_i and ζ_{nano} are the zeta potentials of the oil-water interface and the nanoparticle film of the Janus droplet, respectively. In aqueous solution, ζ_{ow} is negative, while ζ_{nano} is positive[43–46]. Based on Eq. (7), the reduction of nanoparticle coverage of the EIJDs (θ) with the electric field increase leads to both $\bar{\zeta}$ and hence the electrophoretic mobility of the EIJDs decreases. As a result, the increase of the electrokinetic velocity of the EIJDs slows down slightly as the electric field strength increases. When E is larger than 50 V/cm, the effect of electric field on the variation of the nanoparticle coverage is limited; therefore, the electrophoretic velocity increases almost linearly with the electric field.

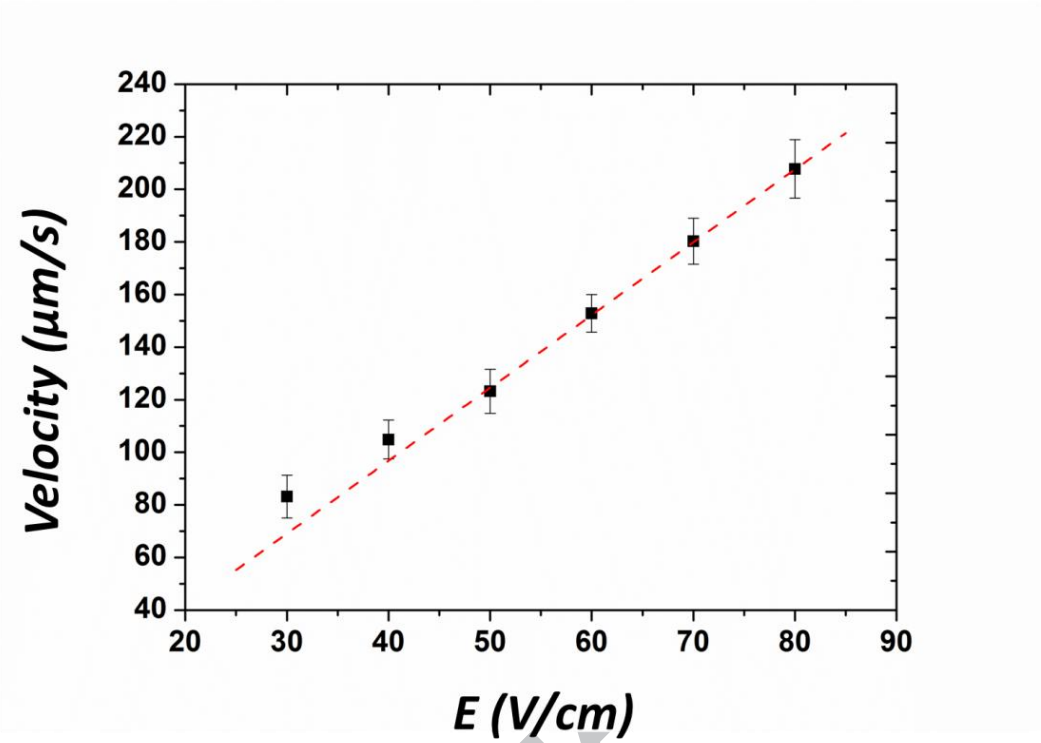

Figure 7. Experimental measured electrokinetic velocities of the EIJDs generated from 1 mg/mL nanoparticle suspension as a function of the electric field. The diameter of the EIJDs ranges from 50 μm to 75 μm.

3.5 Electrokinetic motion of EIJDs under time-varying electric fields

The variation of the electrokinetic velocity of the EIJD fabricated from 1 mg/mL nanoparticle suspension under time-varying electric fields is shown in **Figure 8**. The schematic diagram of the motion of an EIJD in a microchannel under pulsed electric field is shown in **Figure 8(a)**. As the lag of the variation of nanoparticle coverage takes place under time-varying electric fields, the variations of the electrokinetic velocities of the EIJD are different under different electric fields. The variations of the electrokinetic velocity of the EIJD under different time-varying electric fields are shown in **Figure 8(b)** to **(d)**, respectively. The electrokinetic velocities of the EIJD in the increasing period of electric field are shown by the black rectangular points, and those in the decreasing period are shown with the red circular points. As shown in this figures, at

the increasing period, with the increase of the EOF in the microchannel, the electrokinetic velocity increases. However, due the reduction of the nanoparticle coverage of the EIJD as the electric field increases, the electrophoretic mobility decreases gradually. Therefore, the combined electrokinetic velocity increases with gradually decreasing slope. The situation is reversed in the decreasing period, that is, the electrokinetic velocity decreases with increasing rate. This variation of the electrokinetic velocity results from the decrease of the EOF and the increase of the electrophoretic mobility of the EIJD with the decrease of the electric field strength. Due to the lag effect, the nanoparticle coverage of the EIJDs in the increasing period is larger than that in the decreasing period under the same strength of electric field. Hence, the electrokinetic velocity at increasing period is larger. The comparison between **Figure 8(b)**, **(c)** and **(d)** indicates that with the increase of t, the lag effect becomes insignificant, and the difference between the velocities in different periods gets smaller. In the experiments, at least 20 measurements were applied under each condition.

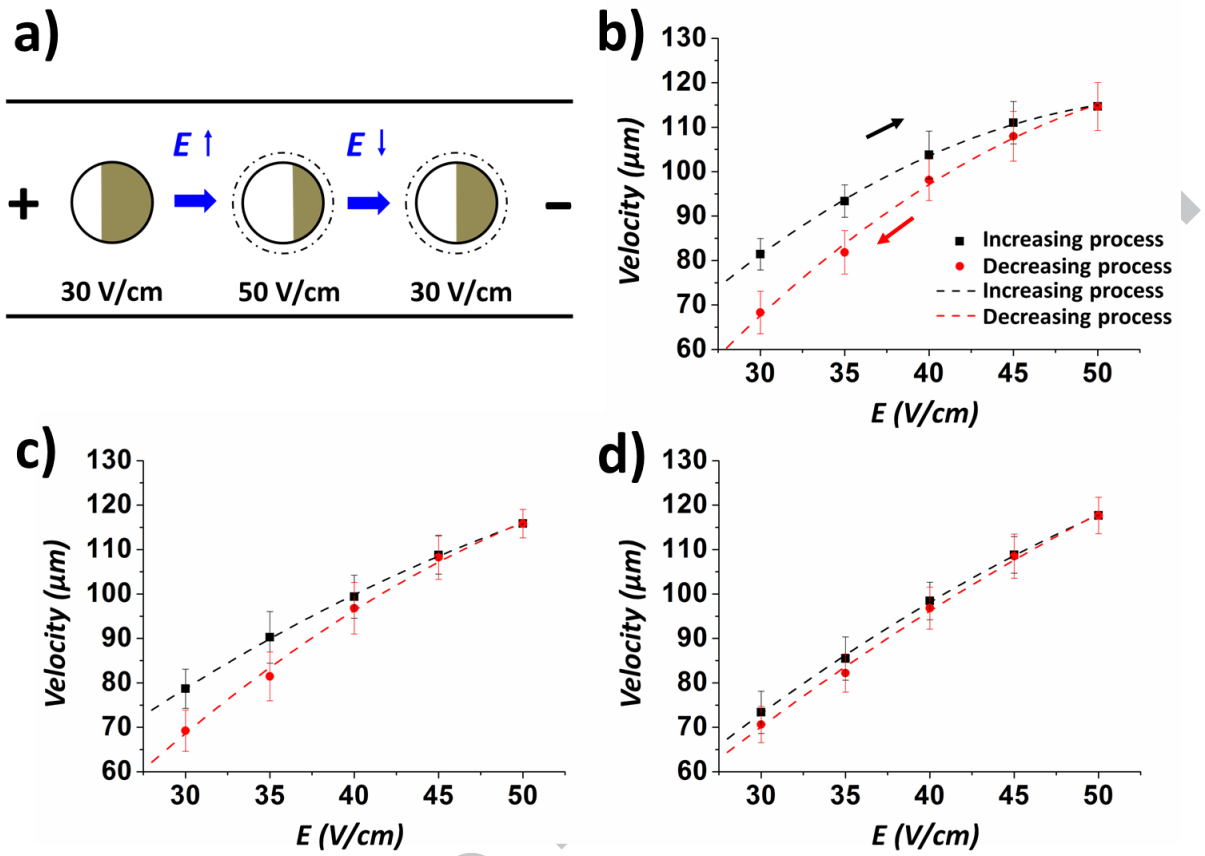

Figure 8. (a) Schematic diagram of the electrokinetic motion of the EIJD under time-varying electric field. **(b)-(c)** The variation of electrokinetic velocities of EIJDs under time-varying electric field with t = 20 s **(b)**, t = 40 s **(c)** and t = 60 s **(d)**. The diameter of the EIJD is approximately 70 μm. The black rectangular points represent the velocities at increasing period of electric field. The red circular points represent the velocities at decreasing period of electric field.

4. Conclusion

The nonlinear electrokinetic motion of EIJDs in a microchannel was studied in this paper. The EIJDs were fabricated by operating aluminum oxide nanoparticles to partially cover one side of the oil droplet under electric field. The nanoparticle coverage of the EIJDs was dependent on the electric field strength. Generally, as the electric field strength increases, the nanoparticle coverage of the EIJDs decreases. Based on the experimental results, an empirical equation was

derived for calculating the nanoparticle coverage as a function of the electric field. The lag of the variation of the nanoparticle coverage of the EIJDs with respect to the applied electric field was studied under different pulsed electric fields. The experimental results indicate that, due to the lag effect, the variation of the nanoparticle coverage is different between the increasing and the decreasing periods of the electric field. The faster the variation of the electric field, the more significant the lag effect. Because of the variation of the nanoparticle coverage of EIJDs, the electrokinetic velocities of EIJDs in a microchannel were affected. As the electric field increases, the electrokinetic velocity of the EIJDs increases while the electrophoretic mobility decreases. Therefore, the electrokinetic velocity of the EIJDs increases nonlinearly with the electric field strength. Under time-varying electric fields, due to the lag effect, the variations of the electrokinetic velocity are different in the increasing and decreasing periods of the electric field. Under the same electric field strength, the electrokinetic velocity of the EIJDs in the increasing period is larger than that in the decreasing period.

Supporting Information

The Supporting Information is available free of charge.

The variation of nanoparticle coverage of the EIJD with the electric field strength (Movie 1.avi)

The evolution of the nanoparticle film of an EIJD with the electric field (Movie 2.avi)

Acknowledgements

The authors wish to thank the financial support of the Natural Sciences and Engineering Research Council (NSERC) of Canada through a research grant (RGPIN-03622) to D. Li.

References

[1] Z. Wu, Y. Gao, D. Li, Electrophoresis 30 (2009) 773–781.

[2] W. Kolch, C. Neusüß, M. Pelzing, H. Mischak, Mass Spectrom. Rev. 24 (2005) 959–977.

[3] M. Ozkan, T. Pisanic, J. Scheel, C. Barlow, S. Esener, S.N. Bhatia, Langmuir 19 (2003) 1532–1538.

[4] L.R. Huang, J.O. Tegenfeld, J.J. Kraeft, J.C. Sturm, R.H. Austin, E.C. Cox, Nat. Biotechnol. 20 (2002) 1048–1051.

[5] J. Fu, R.B. Schoch, A.L. Stevens, S.R. Tannenbaum, J. Han, Nat. Nanotechnol. 2 (2007) 121–128.

[6] C. Ye, X. Xuan, D. Li, Microfluid. Nanofluid. 1 (2005) 234–241.

[7] R. Barchini, D.A. Saville, Langmuir 12 (1996) 1442–1445.

[8] R.F. Probstein, Physicochemical Hydrodynamics: An Introduction, 2nd ed, John Wiley & Sons, New York, 2005.

[9] Y. Kang, D. Li, Microfluid. Nanofluid. 6 (2009) 431–460.

[10] F. Booth, J. Chem. Phys. 19 (1951) 1331–1336.

[11] G.H. Kelsall, S. Tang, S. Yurdakult, A.L. Smith, J. Chem. Soc., Faraday Trans. 92 (1996) 3887–3893.

[12] J.C. Baygents, D.A. Saville, J. Chem. Soc. Faraday Trans. 87 (1991) 1883.

[13] H. Ohshima, J. Colloid Interface Sci. 263 (2003) 333–336.

[14] K. Marinova, R. Alargova, N. Denkov, Langmuir 12 (1996) 2045–2051.

[15] S.A. Nespolo, M.A. Bevan, D.Y.C. Chan, F. Grieser, G.W. Stevens, Langmuir 17 (2001) 7210–7218.

[16] Y. Gu, D. Li, J. Colloid Interface Sci. 206 (1998) 346–349.

[17] Y. Gu, D. Li, Colloids Surfaces A Physicochem. Eng. Asp. 139 (1998) 213–225.

[18] J.L. Anderson, J. Colloid Interface Sci. 105 (1985) 45–54.

[19] M.C. Fair, J.L. Anderson, J. Colloid Interface Sci. 127 (1989) 388–400.

[20] T.H. Hsieh, H.J. Keh, J. Colloid Interface Sci. 315 (2007) 343–354.

[21] H.J. Keh, T.H. Hsieh, Langmuir 24 (2008) 390–398.

[22] J.P. Hsu, H.T. Huang, L.H. Yeh, S. Tseng, Langmuir 28 (2012) 2997–3004.

[23] S. Qian, S.W. Joo, W. Hou, X. Zhao, Society (2008) 5332–5340.

[24] J.P. Hsu, H.T. Huang, L.H. Yeh, S. Tseng, Langmuir 28 (2012) 2997–3004.

[25] A.M. Boymelgreen, T. Miloh, Phys. Fluids 24 (2012).

[26] A.M. Boymelgreen, T. Miloh, Phys. Fluids 23 (2011).

[27] S. Gangwal, O.J. Cayre, M.Z. Bazant, O.D. Velev, Phys. Rev. Lett. 100 (2008) 58302.

[28] T.M. Squires, M.Z. Bazant, J. Fluid Mech. 560 (2006) 65–101.

[29] Y. Daghighi, Y. Gao, D. Li, Electrochim. Acta 56 (2011) 4254–4262.

[30] Y. Daghighi, D. Li, Lab Chip 11 (2011) 2929–2940.

[31] Y. Daghighi, I. Sinn, R. Kopelman, D. Li, Electrochim. Acta 87 (2013) 270–276.

[32] M. Li, D. Li, Electrophoresis 38 (2017) 287–295.

[33] M. Li, D. Li, J. Nanopart. Res. 18 (2016) 120.

[34] M. Li, D. Li, J. Phys. Chem. C 122 (2018) 8461–8472.

[35] M. Li, D. Li, Microfluid. Nanofluid. 21 (2017) 16.

[36] Y. Nakajima, T. Sato, J. Electrostat. 45 (1999) 213–226.

[37] C. Ye, D. Li, J. Colloid Interface Sci. 251 (2002) 331–338.

[38] E.W.K. Young, D. Li, Langmuir 21 (2005) 12037–12046.

[39] E. Bichoutskaia, A.L. Boatwright, A. Khachatourian, A.J. Stace, J. Chem. Phys. 133 (2010) 24105.

[40] J. Stenhammar, P. Linse, H. Wennerström, G. Karlström, J. Phys. Chem. B 114 (2010) 13372–13380.

[41] Y. Gu, J. Colloid Interface Sci. 231 (2000) 199–203.

[42] C. Wang, M. Li, Y. Song, X. Pan, D. Li, Electrophoresis 39 (2017) 807–815.

[43] J.H. Lee, K.S. Hwang, S.P. Jang, B.H. Lee, J.H. Kim, S.U.S. Choi, C.J. Choi, Int. J. Heat Mass Transf. 51 (2008) 2651–2656.

[44] T. Shirai, H. Watanabe, M. Fuji, M. Takahashi, Annu. Rep. Adv. Ceram. Res. Cent. Nagoya Inst. Technol. 9 (2009) 23–31.

[45] V.S. Nguyen, D. Rouxel, R. Hadji, B. Vincent, Y. Fort, Ultrason. Sonochem. 18 (2011) 382–388.

[46] E.S. Basheva, T.D. Gurkov, N.C. Christov, B. Campbell, Colloids Surfaces A Physicochem. Eng. Asp. 282–283 (2006) 99–108.

Graphical Abstract